ELSEVIER

J. Non-Newtonian Fluid Mech. 125 (2005) 61–70

Journal of Non-Newtonian Fluid Mechanics

www.elsevier.com/locate/jnnfm

Asymmetry in the turbulent flow of a viscoelastic liquid through an axisymmetric sudden expansion

C. Dales, M.P. Escudier*, R.J. Poole

University of Liverpool, Department of Engineering (Mechanical Engineering), Brownlow Hill, Liverpool, Merseyside L69 3GH, UK

Received 9 August 2004; received in revised form 7 October 2004; accepted 16 October 2004

Abstract

This paper concerns the asymmetry in mean axial velocity distributions for the flow through an axisymmetric sudden expansion of a viscoelastic, shear-thinning aqueous solution of a polyacrylamide (PAA). The asymmetry manifests itself as an azimuthal variation in the length of the recirculation region of the separated flow downstream of the expansion inlet. For water, the flow is found to be axisymmetric. The asymmetry for the PAA flow, which remained unchanged despite alterations to the flow facility, is attributed to the high viscoelasticity of the polymer solution. The conclusion is drawn that the asymmetry is a purely physical feature of such a flow, and not the product of upstream or downstream flow conditions deriving from the flow facility, or the result of geometrical imperfections in the axisymmetric sudden expansion set-up.
© 2004 Elsevier B.V. All rights reserved.

Keywords: Viscoelastic; Shear thinning; Turbulent; Axisymmetric sudden expansion

1. Introduction

The understanding of turbulence in non-Newtonian fluid flow is limited despite being of immense scientific interest and practical significance. This limitation is directly reflected in the sparseness of literature that reports anything other than fully-developed turbulent flow through channels or pipes in either experimental or theoretical studies, which is unfortunate given the prevalence of non-Newtonian fluid flows in industrial processes that involve synthetic fluids (the food, pharmaceutical and petrochemical industries for example).

The work presented here follows on from a previous study [1] that examined the flow of a viscoelastic fluid through an axisymmetric sudden expansion (ASE). The working fluid was an aqueous solution of a polyacrylamide (PAA), Separan AP273E, which is both shear thinning and viscoelastic. In [1] we investigated the flow for PAA concentrations of 0.02, 0.05 and 0.1% by weight as well as for water. In addition to documenting the increase in reattachment length compared with that for water for the polymer solutions downstream of the expansion—up to three times the length for water for 0.1% PAA—it was also observed that for the highest PAA concentration (and therefore, the most viscoelastic solution) the mean axial velocity profile was no longer axisymmetric. The asymmetry was observed as a difference in the length of the recirculation region on either side of the high velocity jet within the plane of measurement, i.e. an azimuthal variation of the reattachment length. In contrast the asymmetry was not present for water or for lower PAA concentrations and levels of fluid elasticity. These results suggested that the asymmetry was either a purely physical phenomenon of strongly elastic fluid flows, or there are experimental conditions associated with our flow facility (for example geometric imperfections, upstream or downstream flow conditions) that have an accentuated influence on the flow of highly viscoelastic fluids. The latter argument is given credence by the fact that we are unaware of any reports of such asymmetry in ASE geometries prior to [1]. For example Pak et al. [2] presented observations for the flow through an ASE of solutions of the same PAA concentrations as [1] but did not comment on the flow symmetry. It has to be said, however, that since their work was

* Corresponding author. Tel.: +44 151 7944804; fax: +44 151 7944848.
E-mail address: m.p.escudier@liverpool.ac.uk (M.P. Escudier).

0377-0257/$ – see front matter © 2004 Elsevier B.V. All rights reserved.
doi:10.1016/j.jnnfm.2004.10.001

Nomenclature

a	Carreau–Yasuda model parameter
A	area expansion ratio $[(D_P/d_I)^2]$
b	constant in power-law formula for N_1 (Pa^{1-m})
d_I	expansion inlet diameter (m)
D_P	pipe diameter downstream of expansion (m)
D_I	smooth contraction inlet diameter (m)
D_G	diameter of test section glass piping (m)
G'	storage modulus (Pa)
G''	loss modulus (Pa)
h	step height (m)
L	streamwise distance from smooth-contraction inlet (m)
m	power-law index in power-law formula for N_1
n	power-law index in Carreau–Yasuda model
N_1	first normal-stress difference (Pa)
$\dot{Q}$	volumetric flow rate ($m^3\,s^{-1}$)
r	radial distance from centreline (m)
R_P	pipe radius downstream of expansion (m)
R_G	test section glass pipe radius (m)
Re_B	Reynolds number for flow at $x/h = 5$ based on bulk flow Carreau–Yasuda viscosity $[\rho U_B h/\mu_B]$
Re_H	Reynolds number for water $[\rho U_B h/\mu_H]$
Re_M	Reynolds number for flow at $x/h = 5$ based on maximum shear rate Carreau–Yasuda viscosity $[\rho U_B h/\mu_M]$
Re_W	upstream flow Reynolds number based on wall shear rate Carreau–Yasuda viscosity $[\rho U_G D_G/\mu_W]$
U	mean axial velocity ($m\,s^{-1}$)
U_B	expansion inlet bulk velocity $[4\dot{Q}/\pi {d_I}^2]$ ($m\,s^{-1}$)
U_G	bulk velocity in test section glass piping $[4\dot{Q}/\pi {D_G}^2]$ ($m\,s^{-1}$)
x	streamwise distance from expansion (m)
y	radial distance from pipe wall (m)

Greek letters

β	diameter ratio $[D_P/d_I]$
$\dot{\gamma}$	shear rate (s^{-1})
$\dot{\gamma}_B$	expansion bulk flow shear rate $[U_B/h]$ (s^{-1})
$\dot{\gamma}_M$	maximum shear rate at $x/h = 5$ $[(dU/dy)_{max}]$ (s^{-1})
$\dot{\gamma}_W$	laminar approach flow wall shear rate $[(dU/dy)_{wall}]$ (s^{-1})
λ_{CY}	Carreau–Yasuda model time constant (s)
μ	apparent shear viscosity $[= \tau/\dot{\gamma}]$ (Pa s)
μ_B	inlet bulk shear rate Carreau–Yasuda viscosity (Pa s)
μ_{CY}	viscosity corresponding to Carreau–Yasuda model (Pa s)
μ_E	measured shear viscosity (Pa s)
μ_H	shear viscosity of water (Pa s)
μ_M	maximum shear rate at $x/h = 5$ Carreau–Yasuda viscosity (Pa s)
μ_W	wall shear rate Carreau–Yasuda viscosity (Pa s)
μ_0	zero-shear-rate viscosity (Pa s)
μ_∞	infinite-shear-rate viscosity (Pa s)
ρ	fluid density (kg/m^3)
τ	shear stress (Pa)
τ_0	oscillation stress (Pa)
ω	oscillation frequency ($rad\,s^{-1}$)

limited to flow visualisation, it is questionable whether any asymmetry in turbulent flow would be revealed by this technique. Escudier and Smith [3] and Pereira and Pinho [4,5] both reported axisymmetrical mean axial velocity and turbulence intensity profiles for their measurements of the flow of xanthan gum solutions (which are of lower viscoelasticity than the PAA solutions of [1]) downstream of ASE geometries. Castro and Pinho [6] found that the flows of weakly elastic Tylose solutions were also axisymmetric.

It should be emphasised that in contrast to an axisymmetric sudden-expansion flow, asymmetry in a plane sudden expansion (PSE) flow is known to occur above a critical (laminar) Reynolds number. In the plane geometry, a pressure difference is possible between the 'top' and 'bottom' recirculation zones and it is well established [7] for expansion ratios (i.e. ratio of downstream duct height to inlet duct height) greater than 1.5, the separated flows above and below the centreplane interact and result in an asymmetry where one reattachment length is markedly greater than the other. This asymmetry has been observed in both the flow of water [8] and in the flow of highly viscoelastic PAA solutions [9]. As we have shown previously [10], for PSE expansion ratios below 1.5 the reattachment lengths either side of the centreplane are equal and the flow symmetrical, even for highly viscoelastic PAA solutions.

2. Experimental arrangement

A schematic of the flow loop used for this study is shown in Fig. 1 and is broadly the same as that used by Poole and Escudier [1] and by Escudier and Smith [3] for their axisymmetric sudden expansion measurements. The principal alterations were a modification to the expansion module used in [1], and the inclusion of a plenum chamber at the inlet to the test section of the flow loop for some of the measurements reported here (see Section 4.4 below).

Fig. 2 shows a schematic diagram of the axisymmetric sudden expansion. The expansion module comprised a short (135 mm in length) smooth contraction (150 mm concave followed by 75 mm convex radii), located 9.5 m downstream of

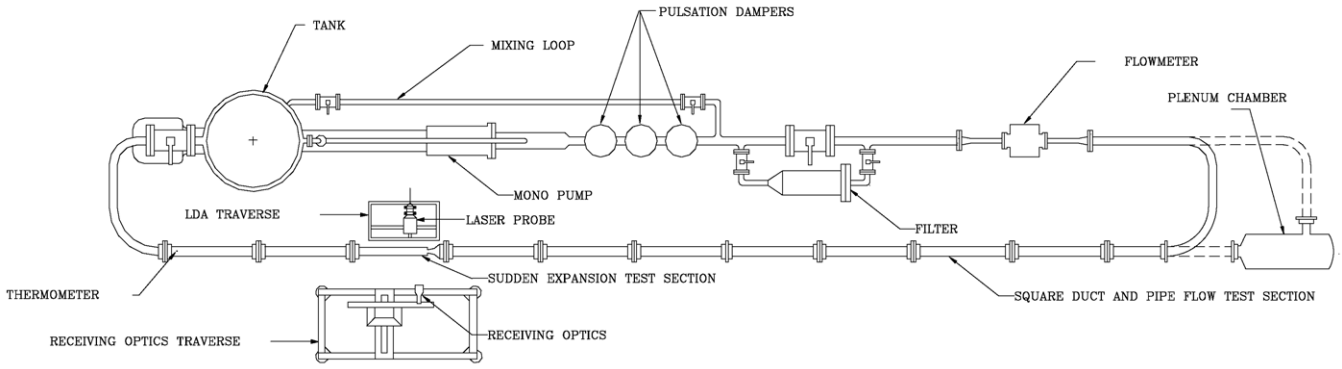

Fig. 1. Schematic diagram of flow facility.

the test section inlet (reduced to 9.2 m with the plenum chamber). The initial internal diameter of the smooth contraction inlet D_I was 100 mm (which matched the internal diameter of the upstream glass piping D_G) and the final internal diameter (i.e. the expansion inlet diameter) d_I was 26 mm. The contraction was followed by a Perspex pipe of internal diameter $D_P = 38.9$ mm, giving an expansion step height $h = 6.45$ mm (compared with $h = 13$ mm in [1]). These dimensions produce an expansion diameter ratio $\beta = D_P/d_I = 1.50$ and expansion area ratio $A = (D_P/d_I)^2 = 2.24$. The 38.9 mm pipe extended for 900 mm until a second sudden expansion back to the 100 mm glass piping, which continued for a further 2 m.

The internal diameter of the 38.9 mm pipe was found to vary azimuthally by ± 0.05 mm and this imparted a measurable out-of-roundness on the expansion conditions. As shown in Fig. 2 this pipe was sealed to the outer diameter of the smooth contraction by a rubber O-ring recessed into the surface of the contraction collar, an arrangement which also ensured that the expansion pipe was coaxial with the smooth contraction (see Section 4.4 below). In addition this arrangement allowed the downstream pipe to be rotated relative to the smooth contraction. The downstream pipe could also be extended to 1800 mm, the outlet being located within the 100 mm glass-piping interior for this configuration.

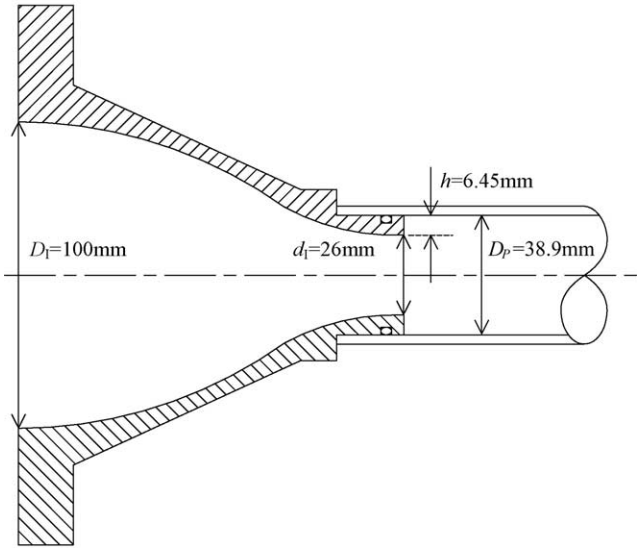

Fig. 2. Axisymmetric sudden expansion (dimensions in mm).

As is also discussed in Section 4.4, for some experiments a cylindrical plenum chamber, 70 L in capacity (720 mm in length, inner diameter 354 mm), was installed to replace the inlet bend to the test section as shown in Fig. 1. The plenum chamber was intended to remove any asymmetry in the flow entering the test section. Within the plenum chamber was a disc of the same diameter equal to the inner diameter of the plenum chamber, with a series of symmetrically-placed holes which combine to give an open area twice that of the plenum chamber exit area (7.85×10^{-3} m^2). Immediately downstream of the plenum chamber inlet was a 90° bend within the plenum interior that directed flow to the rear wall of the chamber. A crossbeam flow straightener was located at the plenum chamber outlet to suppress any residual swirling motions in the fluid entering the test section.

The Dantec Fibreflow laser Doppler anemometer (LDA) system used for the mean velocity measurements comprised a Dantec 60X10 probe and a Dantec 55X12 beam expander in conjunction with a Dantec Burst Spectrum Analyzer signal processor (model 57N10). The beam separation at the front lens was 51.5 mm and the lens focal length 160 mm (corresponding to an included half angle of 9.14°) which produces a measurement volume with principal axis in the radial direction of length 0.21 mm and diameter 20 μm. In view of the small diameter of the measuring volume, no correction was applied for the effect of velocity-gradient broadening. As recommended by Tropea [11], transit-time weighting was used to correct the velocity measurements for the effects of velocity bias. Measurements were taken in forward scatter along a horizontal radial line at $x/h = 5$ (x being the distance downstream of the expansion inlet), starting at the side of the expansion closest to the LDA transmitting optics. For reasons that will become apparent later, it is important to note that all measurements were taken with the transmission optics penetrating the flow from the same side of the pipe. Measurements upstream of the smooth contraction were taken in the same manner at $L/D_G = -1$ and -26 (L measured axially from the

smooth contraction inlet) to examine the approach-flow velocity profile. At each location, nominally 40,000 velocity samples were collected which resulted in a maximum relative statistical error, for a 95% confidence interval, of approximately 0.3% in the mean velocity (Yanta and Smith [12]). The total uncertainty in the mean velocity is estimated to be in the range 3–4%.

The volumetric flow rate $\dot{Q}$ was measured using a Fischer and Porter electromagnetic flow meter (model 10D1) incorporated in the flow loop upstream of the sudden expansion (see Fig. 1) with the flowmeter output signal recorded via an Amplicon PS 30AT A/D converter.

All rheological measurements were carried out using a TA Instruments Rheolyst AR 1000N controlled-stress rheometer. A temperature of 20 °C was maintained for the rheological measurements, which was also the average temperature of the fluid for the duration of the experimental runs. Control of the temperature of the sample to within ±0.1 °C is achieved in the rheometer via a plate using the Peltier effect.

3. Rheology of the working fluid

The working fluid was nominally identical to one of those used in [1], i.e. an aqueous solution of polyacrylamide (PAA), Separan AP273 E supplied by SNF UK limited, concentration 0.1% by weight and optically transparent, thereby permitting LDA measurements. The solvent was filtered tap water with 100 ppm of 40% formaldehyde solution (i.e. 4×10^{-3}% concentration) added to retard bacterial degradation. The average molecular weight for the PAA used in this study, ascertained using gel-phase chromatography, was 1.94×10^6 kg/kmol with a polydispersity of 1.05.

A principal drawback of the PAA solution is its susceptibility to mechanical degradation, which becomes evident in both the shear rheology of the working fluid and in the LDA measurements. Fig. 3 presents the apparent shear viscosity μ versus shear stress τ for a freshly prepared solution of PAA and for the same fluid after progressive shearing. Progressive shearing involved the fluid being pumped around the flow loop at the three flow rates at which LDA measurements were taken (approximately 9.3, 12.3 and 15.3 m^3/h) for a total of 6 h (i.e. 2 h at each flow rate, which is approximately the time taken to complete one LDA traverse of the test section).

Superimposed onto the rheological data in Fig. 3 are the corresponding Carreau–Yasuda model fits:

$$\mu_{CY} = \mu_\infty + \frac{\mu_0 - \mu_\infty}{(1 + (\lambda_{CY}(\tau/\mu_{CY}))^a)^{n/a}} \quad (1)$$

where μ_0 is the zero-shear-rate viscosity, μ_∞ the infinite-shear-rate viscosity, λ_{CY} a time constant, n a power-law index and a parameter introduced by Yasuda et al. [13]. The model parameters, which are listed in Table 1 for both the freshly prepared and progressively sheared measurements, were determined using the fitting procedure outlined in Escudier et al. [14], in essence minimisation of the standard deviation of $(1 - \mu_E/\mu_{CY})^2$, μ_E being the experimental estimate of the shear viscosity. The most noticeable change due to progressive shearing is a 16% reduction of the zero shear rate viscosity μ_0.

The variation of first normal stress difference N_1 with shear stress, which is a good measure of the degree of fluid elasticity, is shown in Fig. 4a for the freshly prepared and pro-

Table 1
Carreau–Yasuda model parameters for 0.1% PAA

Solution status	μ_0(Pa s)	μ_∞(Pa s)	λ_{CY}(s)	n	a
Freshly prepared	4.00	0.00353	43.5	0.658	1.35
Progressively sheared	3.35	0.00343	38.6	0.651	1.11

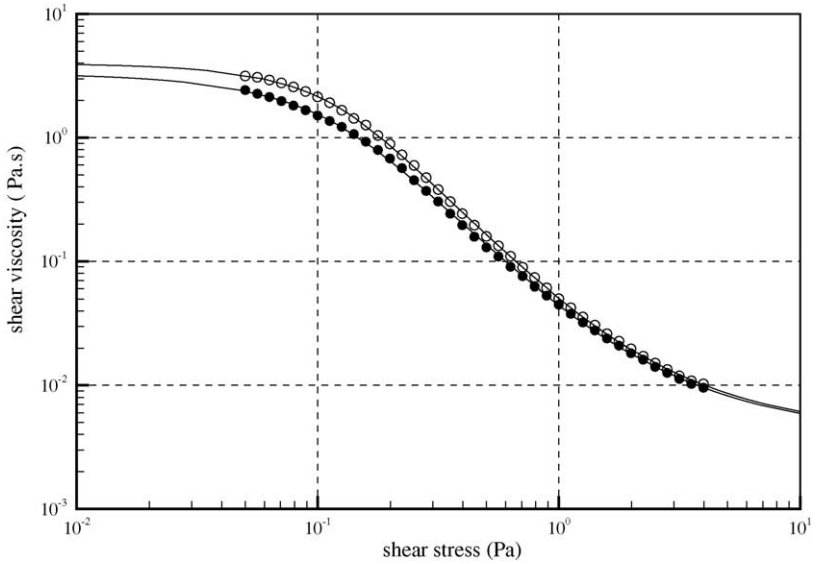

Fig. 3. Viscometric data for freshly prepared (◯) and mechanically degraded (●) 0.1% PAA solution (solid lines are Carreau–Yasuda model fits).

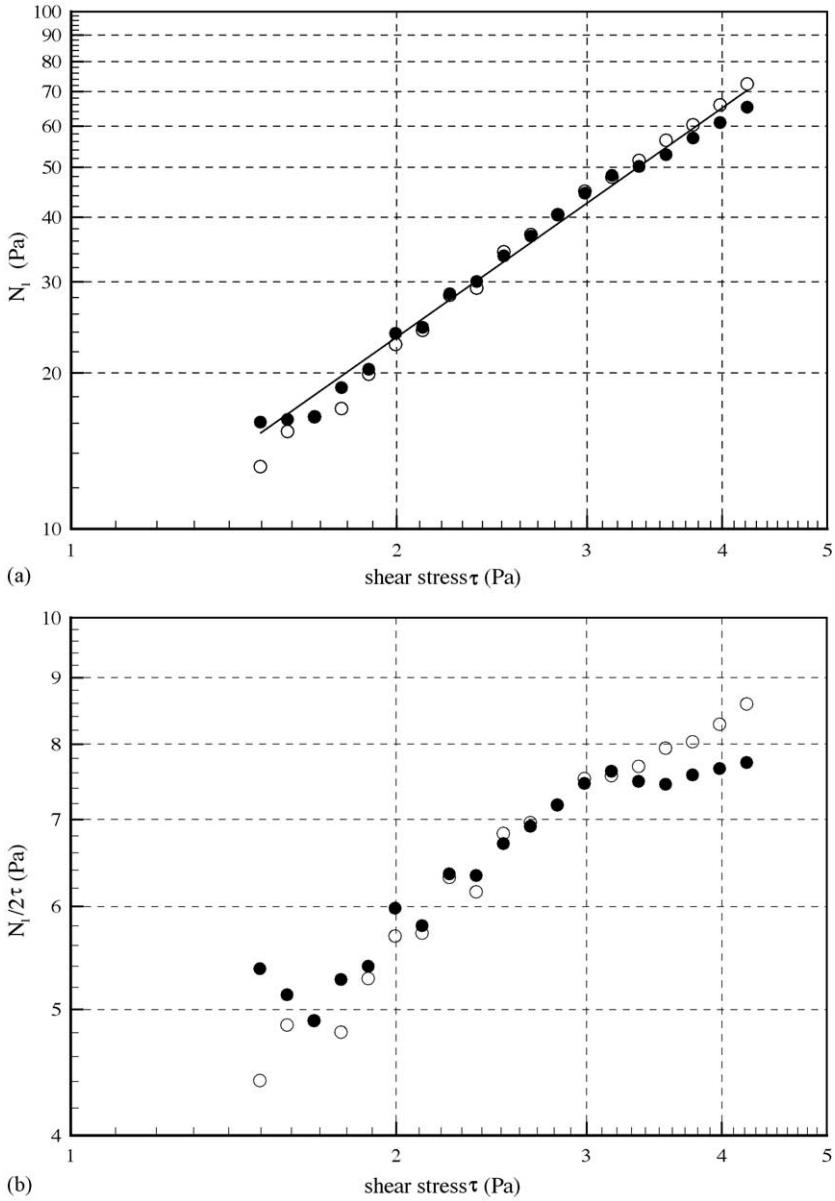

Fig. 4. (a) First normal stress difference for freshly prepared (◯) and mechanically degraded (●) 0.1% PAA solution (solid line is power law fit). (b) Recoverable shear for freshly prepared (◯) and mechanically degraded (●) 0.1% PAA solution.

gressively sheared samples of PAA solution. As can be seen in Fig. 4b, over the measured range the recoverable shear $N_1/2\tau$ for both samples is much greater than 0.5 indicating a highly elastic liquid [15]. No systematic change in N_1 is apparent between the samples within the shear stress range investigated, which cannot extend to the lower shear stresses of the rheology curve in Fig. 3 where the values of N_1 are below the sensitivity of our rheometer. A power-law fit to the N_1 data:

$$N_1 = b\tau^m \tag{2}$$

leads to $b = 8.46\,\mathrm{Pa}^{1-m}$ and $m = 1.47$ over the range $1.5 < \tau < 4.2$.

The storage G' and loss G'' moduli are shown as a function of oscillation frequency ω in Fig. 5, measured at an oscillation stress τ_0 of 0.05 Pa which is well within the linear viscoelastic region of the PAA solution (which was found to lie between $0.01\mathrm{Pa} \leq \tau_0 \leq 0.2$ Pa). As with the N_1 data, no systematic differences between the fresh and progressively sheared samples are evident in this measure of the fluid viscoelasticy.

4. Flow measurements

4.1. Reynolds number for the flow of PAA

Reynolds numbers for mean axial velocity measurements taken downstream of the expansion are defined based upon

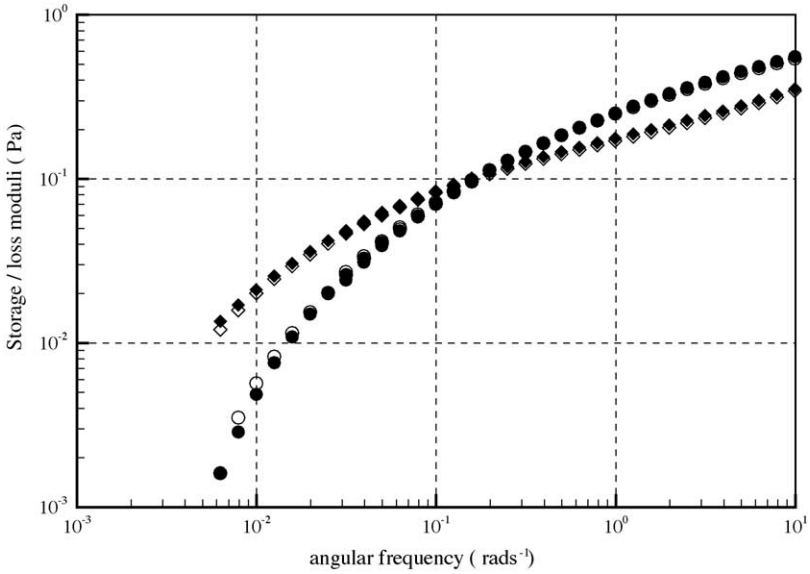

Fig. 5. Storage (◯) and loss (◊) moduli for freshly prepared (open symbols) and mechanically degraded (closed symbols) 0.1% PAA solution.

the bulk velocity at the expansion inlet U_B ($= 4\dot{Q}/\pi d_I^2$) as the velocity scale and the expansion step height h as the length scale. The density of the polymer solution ρ is practically unchanged from that of the solvent (water). A dynamic viscosity μ_B is inferred from the Carreau–Yasuda model for the freshly prepared polymer solution, using a characteristic flow shear rate $\dot{\gamma}_B = U_B/h$. As an alternative, we estimate a viscosity μ_M corresponding to the maximum shear rate $\dot{\gamma}_M = (dU/dy)_{max}$obtained from the velocity distributions at $x/h = 5$. These estimates provide two Reynolds numbers $Re_B = \rho U_B h/\mu_B$ and $Re_M = \rho U_B h/\mu_M$, the latter always being higher due to the shear-thinning nature of PAA.

To define a Reynolds number for the LDA measurements in the 100 mm glass tubing preceding the smooth contraction, we use the bulk velocity U_G in the glass pipe and diameter D_G as the velocity and length scales respectively. A wall shear rate $\dot{\gamma}_W = (dU/dy)_{wall}$ is then estimated from the velocity profiles to provide a viscosity μ_W using the Carreau–Yasuda model. The upstream flow Reynolds number is then $Re_W = \rho U_G D_G/\mu_W$.

4.2. Water flow

Fig. 6 shows the mean axial profile downstream of the ASE at $x/h = 5$ for water flow at two Reynolds numbers $\rho U_B h/\mu_H$ corresponding to inlet bulk velocities of approximately 2.0 and 8.0 m s^{-1}. The local mean axial velocity U is normalised by U_B, and the radial distance from the centreline r by the radius of the pipe downstream of the contraction R_P. The profiles reveal complete symmetry in the plane of measurement, emphasised by the superimposed rotation of the original data about the pipe centreline (i.e. $r/R_P = 0$), and by the solid line which represents the numerically determined average between the actual and rotated data and is included as a reference curve. Despite the four-fold increase in Re there is little quantitative difference between the two profiles. As expected for high Reynolds number flows of a Newtonian fluid through a smooth contraction, the velocity is essentially uniform in the high velocity core ($r/R_P < 0.5$). Both profiles yielded an apparent bulk flow rate (determined by numerical integration) within 5% of the value indicated by the electromagnetic flow meter.

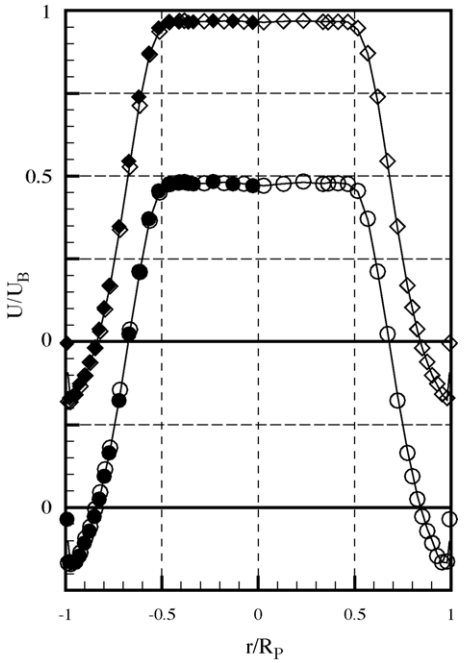

Fig. 6. Axisymmetric flow of water at $x/h = 5$ (closed symbols represent data for $r/R_P > 0$ rotated about $r/R_P = 0$) for $Re_H = 12810$ {◯}; 51360 {◊} (in this and subsequent figures, the solid line represents numerical average between actual data and measurements rotated about $r/R_P = 0$).

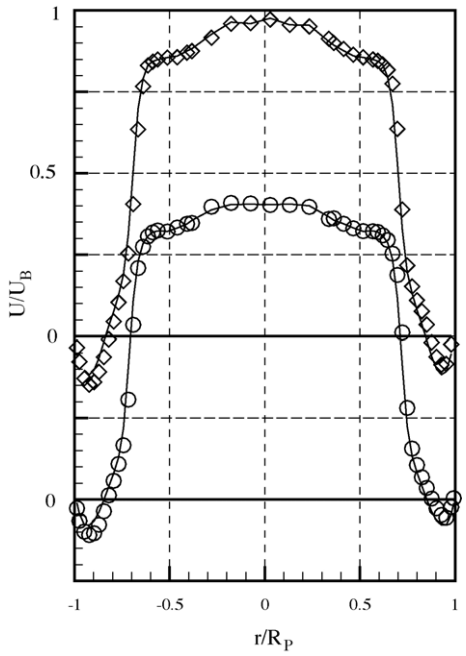

Fig. 7. Mean axial velocity for 0.1% PAA at $x/h = 5$ for Re_B (Re_M) = 5830 (7610) {◯}; 7820 (9870) {◊}.

4.3. 0.1% PAA fluid flow

Fig. 7 shows the mean axial velocity profiles at $x/h = 5$ for 0.1% PAA for inlet bulk flow velocities of approximately 6.4 and 8.0 m s^{-1}. The profiles are symmetrical in the core of the flow ($r/R_P < 0.65$), as revealed by the solid lines. The core diameter is now larger than for the water flow ($0.65D_P$ as opposed to $0.5D_P$). As observed previously [1] there is a bulging of the velocity profile in the core, whereas for water (Fig. 6) the profile in this region remains entirely uniform. For this concentration of PAA, an accelerated central core of uniform velocity is observed with an inflected velocity profile either side flanked by the shear layer. The non-uniform profile on the central core between the shear layers we attribute to the highly-viscoelastic liquid interacting with the smooth contraction, since the effect of shear thinning is normally to flatten the velocity profile. The core velocity profile is also influenced by mechanical degradation of the polymer solution as it is progressively sheared, the principal effect of which we have already shown leads to a reduction in the zero-shear-rate viscosity of the fluid flow curve (Fig. 3). The consequence of degradation on the core velocity is clearly evident in Fig. 8, where the mean axial profile measurements are shown at the same inlet bulk velocity (4.9 m s^{-1} compared with 6.4 and 8.0 m s^{-1} for the data of Fig. 7) prior and subsequent to progressive shearing, and relate directly to the rheological measurements of the same fluid at each state which we discussed

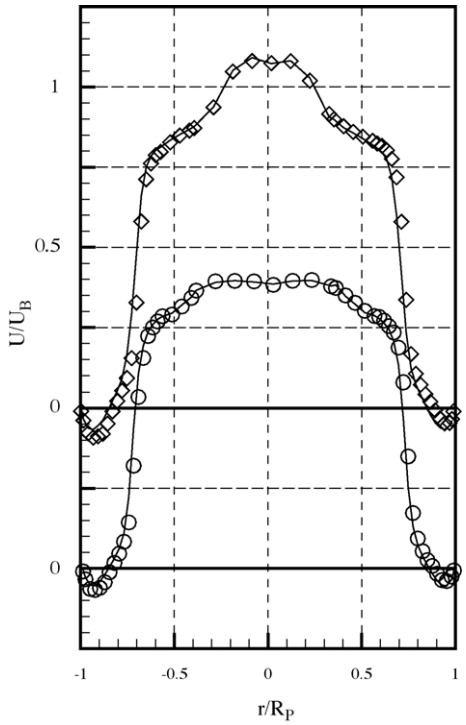

Fig. 8. Mean axial velocity for 0.1% PAA at $x/h = 5$ before (◯) and after (◊) progressive shearing for Re_B (Re_M) = 3930 (5220) {◯}; 3930 (4530) {◊}.

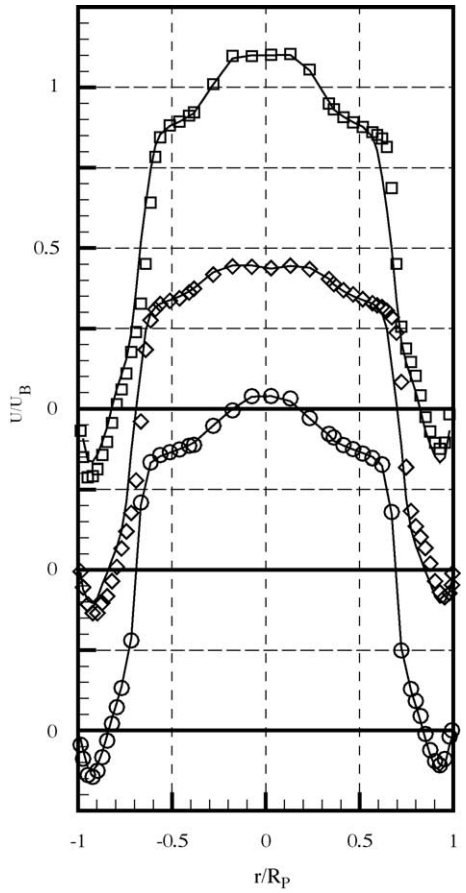

Fig. 9. Mean axial velocity for 0.1% PAA at $x/h = 5$ after modifications to the rig: 180° rotation of downstream pipe, for Re_B (Re_M) = 7860 (10170) {◯}; 180° rotation of contraction 7960 (10170) {◊}; installation of plenum chamber 7960 (9620) {□}.

in Section 3. For the progressively sheared measurements an inner core develops within which the velocity has increased by a further 20% of the bulk velocity. As discussed in [1], the profile shape in the central core is strongly influenced by the gradual contraction and it is this flow which appears to be directly affected by the degradation. In addition the length of the recirculation zone appears to increase in response to the increased acceleration of the fluid in the core for the degraded PAA solution, whereas the gradients in the shear layer remain largely unaltered. We conclude that both the velocity profile and shear viscosity are consistent with polymer degradation in regions of low (tending to zero) shear rate.

We also note a difference between the reattachment lengths of the recirculation regions on either side of the pipe, which is marked by a difference in the minimum negative mean velocity in the separated flow either side of the high velocity core within the plane of measurement. The degree of asymmetry is noted to increase with *Re* but remain in the same sense for both sets of measurements in Fig. 7, and is also evident in the pre- and post-shearing results of Fig. 8. From the foregoing we conclude that the asymmetry in Figs. 7 and 8 is either a purely physical phenomenon of such highly elastic flows (i.e. perhaps an instability related to the relative levels of elasticity, inertia and viscosity), or it is a feature peculiar to our flow facility that becomes apparent only for highly elastic flows. In the case of the latter, one possibility is that the asymmetry is a product of imperfections in the flow geometry within the vicinity of the sudden expansion which interact with the highly viscoelastic solution. A second possibility is that the velocity profiles within the expansion are influenced by either upstream or downstream flow conditions. As noted in Section 2, the LDA system was operated in forward-scatter mode with the transmission optics always on the same side of the pipe. If the optical arrangement of the LDA system were to be responsible for the asymmetry we observed, it would have to be the case that the asymmetry would be seen in all measurements. As can be seen from Fig. 6, no asymmetry was found for the two water flows, and the LDA system itself has to be excluded from consideration. It is also the case that the level of uncertainty in the measurements, at most 4% of the local mean velocity, is far too low to give rise to an appearance of asymmetry, either within the regions of reversed flow or the radial shift of the central core.

4.4. Examining the source of asymmetry for the flow of 0.1% PAA

To investigate which, if any, of the influences suggested above are responsible for the flowfield asymmetry, a series of measurements was undertaken following modifications to the flow facility: 180° rotation of the 38.9 mm pipe; 180° rotation of the smooth contraction; installation of an upstream plenum chamber; doubling the length of the 38.9 mm pipe. The results for the first three modifications are shown in Fig. 9 and it is evident that none of them affects either the sense of the asymmetry within the recirculation region or the reattachment lengths. However, in the case of rotation of the downstream pipe, the axisymmetry of the central region is greatly

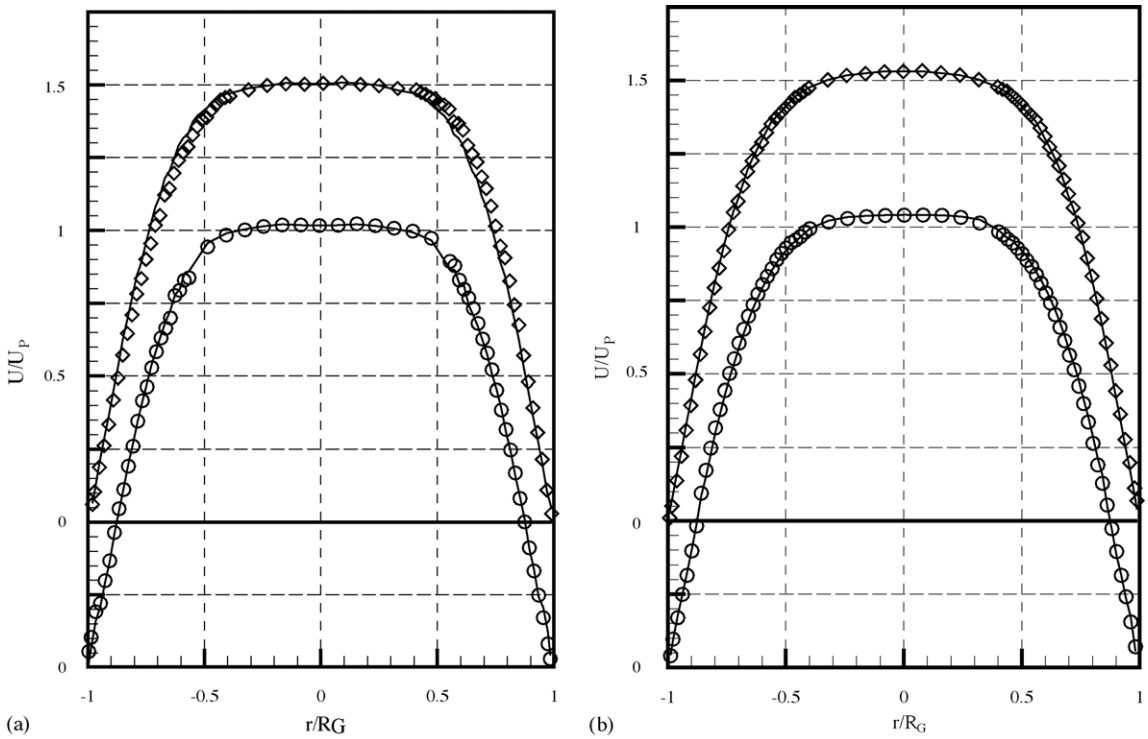

Fig. 10. (a) Laminar approach flow of 0.1% PAA in 100 mm pipe for $Re_W = 1700$ at locations $L/D_G = -1$ {◯}; $= -26$ {◊} prior to plenum chamber installation. (b) Laminar approach flow of 0.1% PAA in 100 mm pipe for $Re_W = 1700$ at locations $L/D_G = -1$ {◯}; $= -26$ {◊} after plenum chamber installation.

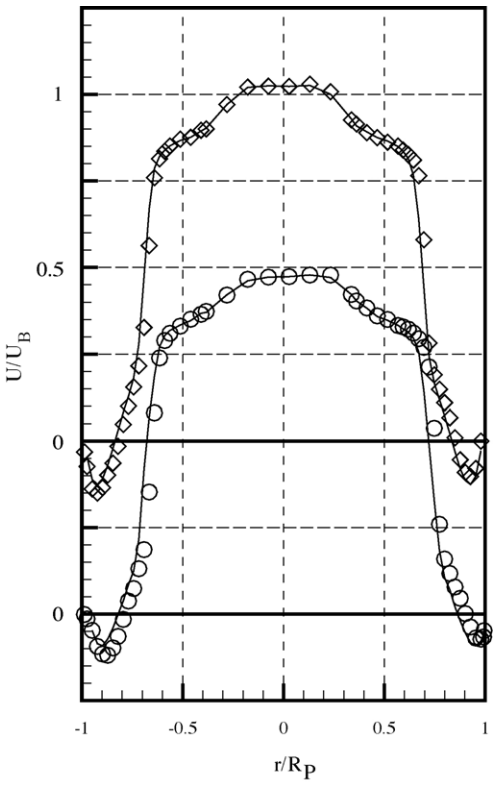

Fig. 11. Mean axial velocity of 0.1% PAA with extension of downstream (38.9 mm Ø) pipe at $x/h = 5$ for Re_B (Re_M) = 5760 (7500) {◯} and 7740 (10050) {◇}.

improved although asymmetry in the reversed-flow regions remains, where the difference in magnitude between the minimum velocities in either region (as a percentage of the average of the two values) is about 30%, i.e. far from negligible. In addition we note that the plenum chamber was effective in removing a slight asymmetry in the laminar approach-flow (upstream of the smooth contraction) that appears to amplify towards the test-section entrance. The approach-flow asymmetry is evident in Fig. 10a for axial velocity measurements at $L/D_G = -26$ (relative to the smooth contraction inlet) which diminishes (but is still apparent) at $L/D_G = -1$. By contrast the asymmetry is no longer perceptible at the same upstream locations in Fig. 10b with the plenum chamber installed.

The fourth modification altered the downstream flow conditions by doubling the length of the 38.9 mm pipe into which the flow first expands, thus diminishing any possible upstream effects a second sudden expansion might impose on the mean axial flow at the inlet. For the flow of a Newtonian fluid through a plane sudden expansion (PSE) Mullin et al. [16] observed that a slight contraction placed some distance downstream of the inlet imparted an upstream influence by altering the critical Reynolds number at which the flow became asymmetric. As revealed in Fig. 11, for our ASE geometry this final modification also had no influence on the asymmetry at $x/h = 5$, which remained unchanged from that of Fig. 7 for the same bulk inlet velocities.

In summary, none of the modifications to the flow facility have influenced the asymmetry; the asymmetry is not observed in water, in weaker PAA solutions [1] or in other polymer solutions of lower viscoelasticity (xanthan gum in [3–5] or Tylose in [6]); and the asymmetry is unaffected by flowrate (note that the majority of measurements were taken for bulk flow velocities of 6.4 and 8.0 m s^{-1} but those of Fig. 8 were for the lower velocity of 4.9 m s^{-1}).

5. Conclusions

We have sought to identify the source of asymmetry apparent in the mean axial velocity measurements of a highly elastic polymer solution (0.1% PAA) downstream of an axisymmetric sudden expansion. The asymmetry contrasts with the axisymmetric flow of water at two Reynolds numbers through the same geometry. Our results lead us to conclude that geometrical imperfections in the sudden expansion test module are not the source of asymmetry in the flow of the PAA solution. Neither can the asymmetry be ascribed to the flow conditions at inlet to the upstream piping which produce a slight but measurable asymmetry in the laminar approach flow velocity profile (removed by installing a plenum chamber at the entrance to the test section), or the presence of a second sudden expansion at the test module exit, which we distanced from the region of measurement by extending the pipe into which the flow enters after the first expansion inlet.

Our LDA measurements downstream of the axisymmetric sudden expansion for the flow of the 0.1% PAA highlighted the influence of mechanical degradation of this fluid. The degradation leads to an increased overshoot in the mean axial velocity in the core of the flow, and correlates with a reduction in the zero shear rate viscosity of the degraded liquid. Measurements of the first normal stress difference and the storage and loss moduli show no perceptible change in the measurable range due to mechanical degradation.

References

[1] R.J. Poole, M.P. Escudier, Turbulent flow of viscoelastic liquids through an axisymmetric sudden expansion, J. Non-Newt. Fluid Mech. 117 (2004) 25–46.
[2] B. Pak, Y.I. Cho, S.U.S. Choi, Separation and reattachment of non-Newtonian fluid flows in a sudden expansion pipe, J. Non-Newt. Fluid Mech. 37 (1990) 175–199.
[3] M.P. Escudier, S. Smith, Turbulent flow of Newtonian and shear-thinning liquids through a sudden axisymmetric expansion, Exp. Fluids 27 (1999) 427–434.
[4] A.S. Pereira, F.T. Pinho, Turbulent characteristics of shear-thinning fluids in recirculating flows, Exp. Fluids 28 (2000) 266–278.
[5] A.S. Pereira, F.T. Pinho, The effect of the expansion ratio on a turbulent non-Newtonian recirculating flow, Exp. Fluids 32 (2002) 458–471.
[6] O.S. Castro, F.T. Pinho, Turbulent expansion flow of low molecular weight shear-thinning solutions, Exp. Fluids 20 (1995) 42–55.

[7] D.E. Abbott, S.J. Kline, Experimental investigation of subsonic turbulent flow over single and double backward facing steps, J. Basic Eng. D 84 (1962) 317–325.
[8] M.P. Escudier, P.J. Oliveira, R.J. Poole, Turbulent flow through a plane sudden expansion of modest aspect ratio, Phys. Fluids 14 (2002) 3641–3654.
[9] R.J. Poole, M.P. Escudier, Turbulent flow of a viscoelastic shear-thinning liquid through a plane sudden expansion of modest aspect ratio, J. Non-Newt. Fluid Mech. 112 (2003) 1–26.
[10] R.J. Poole, M.P. Escudier, Turbulent flow of non-Newtonian liquids over a backward-facing step. Part II. Viscoelastic and shear-thinning liquids, J. Non-Newt. Fluid Mech. 109 (2003) 193–230.
[11] C. Tropea, Laser Doppler anemometry: recent developments and future challenges, Meas. Sci. Technol. 6 (1995) 605–619.
[12] W.J. Yanta, R.A. Smith, Measurements of turbulence-transport properties with a laser-Doppler velocimeter, in: Proceedings of the 11th Aerospace Science Meeting, AIAA Paper 73, Washington, 1973, pp. 169–179.
[13] K. Yasuda, R.C. Armstrong, R.E. Cohen, Shear flow properties of concentrated solutions of linear and star branched polystyrenes, Rheo. Acta 20 (1981) 163–178.
[14] M.P. Escudier, I.W. Gouldson, A.S. Pereira, F.T. Pinho, R.J. Poole, On the reproducibility of the rheology of shear-thinning liquids, J. Non-Newt. Fluid Mech. 97 (2001) 99–124.
[15] H.A. Barnes, J.F. Hutton, K. Walters, An Introduction to Rheology, Elsevier, 1989.
[16] T. Mullin, S. Shipton, S.J. Tavener, Flow in a symmetric channel with an expanded section, Fluid Dyn. Res. 33 (2003) 433–452.